# Color control through plasmonic metal gratings

M. A. Vincenti, M. Grande, D. de Ceglia, T. Stomeo, V. Petruzzelli et al.

Citation: Appl. Phys. Lett. **100**, 201107 (2012); doi: 10.1063/1.4718764
View online: http://dx.doi.org/10.1063/1.4718764
View Table of Contents: http://apl.aip.org/resource/1/APPLAB/v100/i20
Published by the American Institute of Physics.

# Color control through plasmonic metal gratings

M. A. Vincenti,[1,a)] M. Grande,[2] D. de Ceglia,[1] T. Stomeo,[3] V. Petruzzelli,[2] M. De Vittorio,[3,4] M. Scalora,[5] and A. D'Orazio[2]
[1]*AEgis Technologies Group, 410 Jan Davis Drive, Huntsville, Alabama 35806, USA*
[2]*Dipartimento di Elettrotecnica ed Elettronica, Politecnico di Bari, Via Re David 200, 70125 Bari, Italy*
[3]*Italian Institute of Technology (IIT), Center for Bio-Molecular Nanotechnology, Via Barsanti, Arnesano (Lecce) 73010, Italy*
[4]*National Nanotechnology Laboratory (NNL), CNR-Istituto di Nanoscienze, Dip. Ingegneria dell'Innovazione, Università Del Salento, Via Arnesano, 73100 Lecce, Italy*
[5]*Charles M. Bowden Research Center, RDECOM, Redstone Arsenal, Alabama 35898-5000, USA*

(Received 17 October 2011; accepted 1 May 2012; published online 16 May 2012)

We experimentally demonstrate the color tuning abilities of two-dimensional periodic arrays of gold nano-patches on silicon substrate. We observe that changes in the geometrical parameters of the array can shift significantly the plasmonic resonance that occurs at the edge of the plasmonic band gap. Experimental proof of this shift is provided by the observation of an important change in the color of the diffracted field. Calculations of the diffracted spectra match the observed color changes very well and provide an efficient means for the design of sensing platforms based on color observation. © *2012 American Institute of Physics*. [http://dx.doi.org/10.1063/1.4718764]

Since the first observation of surface plasmon resonances,[1] the extreme sensitivity of these surface waves to environmental changes has stimulated the interest of the scientific community for the great potential for sensing applications.[2–7] Several configurations of surface-plasmon-based sensors have been investigated, mostly based on field-enhancement in sub-wavelength regions, namely, nanocavities, nanoparticles, nano-antennas, and nanoclusters, etc.[8–12] Surface plasmons are deemed to play a prominent role in the extraordinary transmission of light in metal gratings with sub-wavelength features,[13] and the formation of a *plasmonic band gap*.[14–16] While a lot has already been said about guided surface plasmons and their applications, one should not lose sight of the considerable instrumentation needed to detect the excitation of such surface modes and eventually monitor their spectral shift. But it is also true that sensing devices relying on localized surface plasmon resonances offer a simplified detection approach based on a direct observation of scattered fields.[17–19] In this letter, we propose an alternative detection scheme based on the measurement of diffraction efficiencies in plasmonic metal gratings. We experimentally monitored color changes of the reflected, diffracted field from two-dimensional arrays of gold nano-patches grown on silicon substrate and found an almost perfect correspondence between the simulated diffraction spectra and the observed color. This proof-of-principle experiment paves the way for yet unexplored plasmonic sensor devices that may eventually help to determine the presence of certain chemicals species or other foreign substances on the surface of a device, without resorting to additional instrumentation.

It is well known that periodically milled slits in metal films lead to peculiar resonant features in their transmitted and reflected spectra.[15,20,21] It has been proven both theoretically and experimentally that the spectral position of surface-plasmon-related features may be linked either to the geometrical parameters of the structure or to the optical properties of the dielectric material adjacent to the metal.[15,20,22] A change in refractive index of the dielectric medium induces a modulation of the effective refractive index of the surface plasmon supported by that interface. The same effect may also be achieved by modulating the geometrical parameters of the grating. For example, let us consider the center of the *plasmonic band gap*.[14–16] The formation of this forbidden band, which is associated with the coupling and back radiation of the unperturbed surface plasmon of the metal/dielectric interface, occurs every time the following condition is satisfied:

$$\lambda_{sp} = \frac{\lambda_0}{n_{spp}} = \frac{p}{m}, \tag{1}$$

where $n_{spp} = \Re\left(\sqrt{\frac{\varepsilon_m \varepsilon_d}{\varepsilon_m + \varepsilon_d}}\right)$ (Ref. 23), $\varepsilon_m$ and $\varepsilon_d$ are the real part of the dielectric permittivities of the metal and dielectric material, respectively, $p$ is the periodicity of the array, $m$ is an integer number, $\lambda_0$ and $\lambda_{sp}$ are the vacuum wavelength and the surface plasmon effective wavelength, respectively. From Eq. (1) one can easily infer that a reduction of the effective wavelength of the surface plasmon can be induced by either an increase of the refractive index of the dielectric material $\varepsilon_d$ or by a reduction of the periodicity of the array. Moreover, the shift of these features corresponds to a dramatic change in the spectrum of all the diffraction orders of the array, which produces significant change in the color of the structure when seen through a dark field (DF) microscope with the naked eye or a commercial camera.

We fabricated a variety of 2D-periodic arrangements of gold patches on silicon by means of electron beam lithography, followed by thermal evaporation and lift-off processes, with the aim to find an accessible way to monitor changes in the environment, such as the presence of biochemical agents. In particular, we report the results relative to two different

a)Electronic mail: mvincenti@aegistg.com.

 

samples, all grown on a 200 nm-thick gold film, having the following geometrical parameters: (i) $a = 120$ nm, $p = 630$ nm, (ii) $a = 160$ nm, $p = 560$ nm, where $a$ is the width of the slits and $p$ is the periodicity of the array. All samples have the same periodicity in both directions (square patches). This choice is not accidental since this is the only condition for which the 2D-periodic structure behaves as the 1D-periodic equivalent (1D array of slits), regardless of the polarization of the incident light.[24,25] It is worth stressing that such a simplification significantly reduces computational burden and computer memory issues.

The 2D patterns have been written using a Raith150 e-beam lithography system operating at 30 kV. A bi-layer, composed of a 500 nm-thick polymethylmethacrylate-methacrylic acid (PMMA-MA) and 200 nm-thick PMMA layers, was adopted as positive resist to ensure good resolution of e-beam writing. The total thickness of the resist layer was chosen to facilitate the lift-off process thus avoiding the presence of resist in the slits. Moreover the bi-layer configuration allowed the fabrication of totally square metal patches with well-controlled geometrical feature sizes easily reproducible with simulations. A proximity error correction (PEC) has been employed in order to achieve identical patches within the single periodic array while a preliminary dose-test has been performed to identify the correct electron dose determined through scanning electron microscope (SEM) inspections. The patterned resist has been used as a mask for the evaporation of the 200 nm-thick gold layer by means of a thermal evaporator with a current of 300 A and a deposition rate of 2 Å/s. It is worth pointing out that the adhesion between the gold layer and the silicon substrate has been aided with the introduction of a 5 nm-thick chrome layer. Finally, a lift-off process in an acetone bath was employed to remove the resist regions and reveal the final 2D array. Figure 1(a) shows the SEM image of one of the devices ($a = 120$ nm, $p = 630$ nm). The roughness of the evaporated gold layer was estimated by means of an atomic force microscope (AFM), obtaining a root mean square value of about 6 nm.

All the fabricated samples have been characterized by means of the optical setup sketched in Fig. 1(b). A white light lamp, with a pass band between 400 and 700 nm, was focused on the sample by means of a low numerical-aperture infinity-corrected microscope objective (10×, NA = 0.25). Since we are interested in monitoring light diffraction in the far field, a microscope in dark field configuration mode was used to investigate the scattering behavior of the periodic structures.

We began our investigation by simulating the 1D-periodic equivalent of samples (i) and (ii) with the aim to find a way to predict the reflected, diffracted spectra of the samples and, as direct consequence, to develop a tool to design sensing platforms based only on color observation. All simulations were performed using a rigorous coupled wave analysis (RCWA) code, validated using a commercial finite element method (FEM) by Comsol Multiphysics. FEM simulations were used also to confirm the equivalent spectral behavior of 2D- and 1D-periodic gratings. Since the DF microscope suppresses the zeroth diffraction order of the array almost completely, we calculated the diffraction efficiencies of all the non-zero diffracted orders that fall within the visibility cone of the microscope. The diffraction orders that contribute to the scattered field could not be the same for all samples since they depend on array periodicity, angle, and wavelength of incident light. In the measurements reported below, the color of samples (i) and (ii) were recorded with an incident light beam incident at $\sim 14^\circ$ onto the samples. From the grating equation $p(\sin\vartheta_m + \sin\vartheta_{in}) = m\lambda_0$, where $\vartheta_{in}$ and $\vartheta_m$ are the incident and the $m$th-order diffracted angles, one can easily conclude that the diffraction order available in the visibility cone of the DF microscope will be only $m = -1$. As mentioned above, the roughness of the sample is not negligible. In order to take into account roughness contributions to the diffraction efficiency, the field scattered from the gold film without slits was measured by collecting the reflected light with an aspherical fiber lens collimator whose signal is sent to an optical spectrometer (HR4000 from Ocean Optics) with an integrated CCD-array detector that enables an optical resolution of about 1 nm through a multimode optical fiber. The measured spectrum is reported in Fig. 2(a). At the same time we observed and recorded the color of the gold film (Fig. 3(a) inset M) by means of a beam splitter (see Fig. 1(b)). We then converted the measured spectrum into the CIE 1931 standard map (black marker in Fig. 3(a)). A zoom of the area associated with the zone of the map indicated by the marker is provided in Fig. 3(a), inset S. The quantification of the contribution coming from the roughness of gold, which represents a systematic error in the observation of our samples, helped us to properly reproduce the scattered field of the other samples in the simulations. Figures 2(b) and 2(c) show the diffracted spectra of the order m = −1 of the gratings, where the measured gold contribution was added. As previously done for the plain gold film, we then compared the color observed through the microscope and recorded with the camera (see insets M in Figs. 3(b) and 3(c)) with the

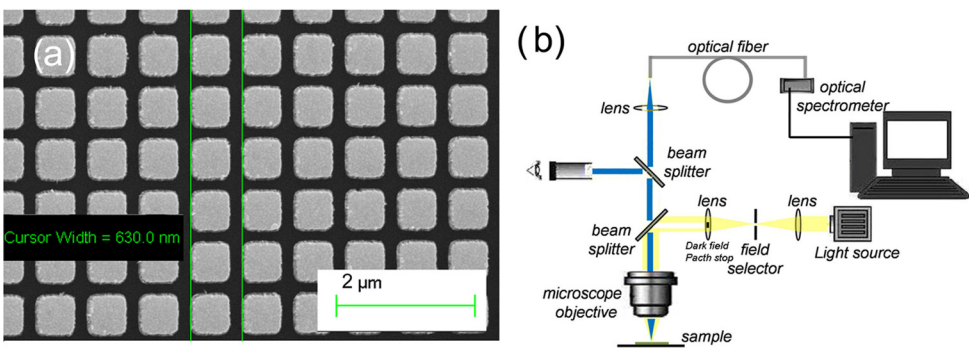


FIG. 1. (a) SEM image of the fabricated device. (b) Sketch of the optical set-up: the yellow and the blue lights correspond to the incident and the scattered lights, respectively.

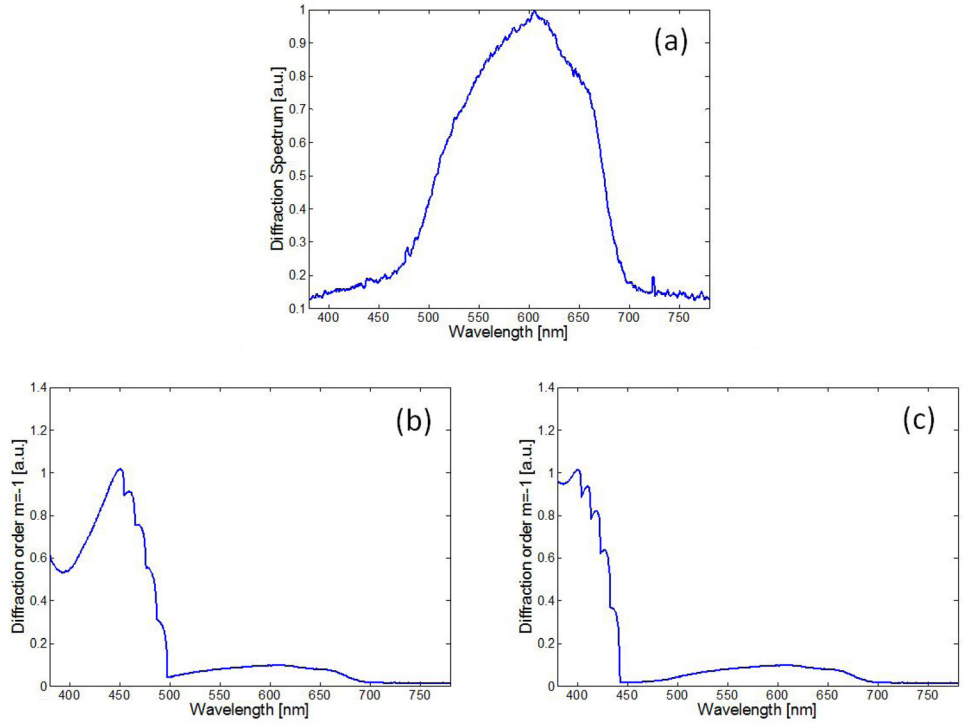


FIG. 2. (a) Measured scattering spectra of 200 nm gold layer. (b) Simulated diffraction efficiency in the field of view of the DF microscope of 1D-periodic arrangement of slits in 200 nm thick gold film with $a = 120$ nm and $p = 630$ nm; (c) same as in (b) with $a = 160$ nm and $p = 560$ nm.

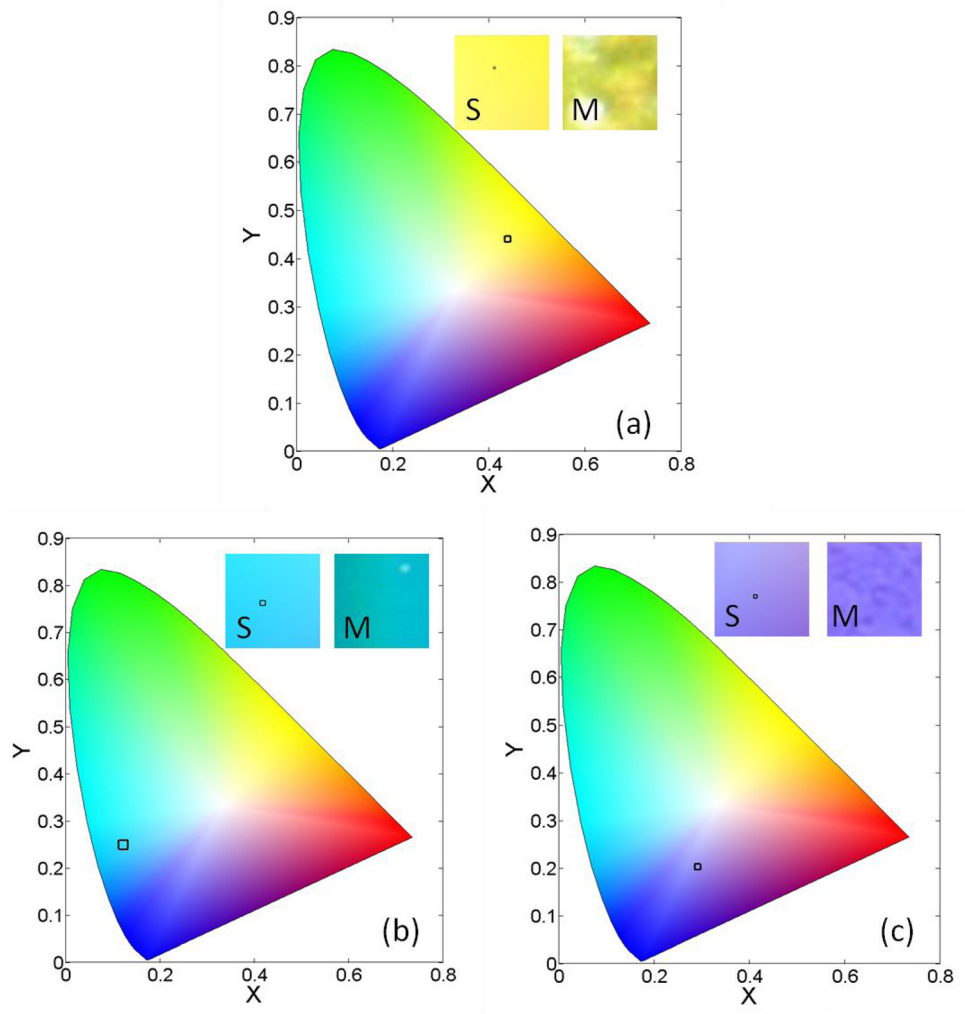


FIG. 3. (a) Comparison of observed color and simulated spectra converted into the CIE 1931 standard map for a plain, 200 nm-thick gold layer (the simulated color is indicated by the black marker on map and inset S, while the observed color is indicated by inset M); (b) same as in (a) for a 1D-periodic arrangement of slits in 200 nm thick gold film with $a = 120$ nm and $p = 630$ nm; (c) same as in (b) with $a = 160$ nm and $p = 560$ nm.

simulated spectra (in Figs. 2(b) and 2(c)) converted into the CIE 1931 standard map. Figures 3(b) and 3(c) provide clear evidence of a very good match of the diffracted spectra (simulated) with the corresponding observed colors (measured). We note that in the simulations of our diffracted spectra in Figs. 2(b) and 2(c) we averaged the incident field between 10° and 14° for sample (i), while for sample (ii) agreement with the observed color was found when averaging was done between 12° and 16°. This small discrepancy between the two measurements may be attributable to two main reasons. One is that the microscope illuminates the sample with a cone of angles centered at 14° which is related to the numerical aperture (NA) of the microscope objective (0.25 in this case); in other words, since the illumination has an annulus shape, it is reasonable to consider a set of angles (instead of a single angle) in the calculation of the diffracted spectra. Second, a slight change in the incident angle may be consequence of slight shifts in the actual working distance between the microscope and the sample in the two separate measurements.

In conclusion we experimentally verified significant changes in the color of the diffracted field associated with changes in the geometrical parameters of 2D-periodic arrangements of square gold patches grown on silicon. The spectra of the diffracted fields were simulated and then converted into their color equivalent into a CIE 1931 standard map. The near perfect correspondence between the simulated spectra and the observed color suggests that a simple, effective approach to plasmonic-based sensing techniques is possible, where a microscope or even the observation with the naked eye may suffice to determine the presence of foreign materials on the device. The measured color shifts and simulated spectra suggest that a sensor based on the proposed technology has sensitivity as high as ~500 nm/RIU, comparable or better than other sensors based on 2D photonic crystal technologies,[26] or ring resonators.[27–29] We also envision the possibility to develop a simple tool to design and predict slight color changes associated with different concentrations of certain materials. For example this approach may be important whenever the target molecules are suspended in a generic biological liquid (analyte) that comes in contact with the surface of the grating.

M.G. acknowledges partial financial support from the Army Research Office (W911NF-11-1-0284-1490-AM-01). The authors would like to acknowledge G. Morea and G. Epifani for support in sample fabrication and measurements.

[1]R. H. Ritchie, Phys. Rev. **106**, 874–881 (1957).
[2]S. Herminjard, L. Sirigu, H. P. Herzig, E. Studemann, A. Crottini, J. P. Pellaux, T. Gresch, M. Fischer, and J. Faist, Opt. Express **17**, 293–303 (2008).
[3]B. Gauvreau, A. Hassani, M. F. Fehri, A. Kabashin, and M. Skorobogatiy, Opt. Express **15**, 11413–11426 (2007).
[4]J. Homola, S. S. Yee, and G. Gauglitz, Sens. Actuators B: Chem. **54**, 3–15 (1999).
[5]B. Nikoobakht, J. Wang, and M. A. El-Sayed, Chem. Phys. Lett. **366**, 17–23 (2002).
[6]F. J. Garcia-Vidal and J. B. Pendry, Phys. Rev. Lett. **77**, 1163–1166 (1996).
[7]A. Kocabas, G. Ertas, S. S. Senlik, and A. Aydinli, Opt. Express **16**, 12469–12477 (2008).
[8]Y. Sonnefraud, N. Verellen, H. Sobhani, G. A. Vandenbosch, V. V. Moshchalkov, P. V. Dorpe, P. Nordlander, and S. A. Maier, ACS Nano **4**, 1664–1670 (2010).
[9]F. Hao, Y. Sonnefraud, P. V. Dorpe, S. A. Maier, N. J. Halas, and P. Nordlander, Nano Lett. **8**, 3983–3988 (2008).
[10]J. B. Lassiter, H. Sobhani, J. A. Fan, J. Kundun, F. Capasso, P. Nordlander, and N. J. Halas, Nano Lett. **10**, 3184–3189 (2010).
[11]W. Zhang, L. Huang, C. Santschi, and O. J. F. Martin, Nano Lett. **10**, 1006 (2010).
[12]W. Kubo and S. Fujikawa, Nano Lett. **11**, 8–15 (2011).
[13]T. W. Ebbesen, H. J. Lezec, H. F. Ghaemi, T. Thio, and P. A. Wolff, Nature (London) **391**, 667–669 (1998).
[14]R. H. Ritchie, E. T. Arakawa, J. J. Cowan, and R. N. Hamm, Phys. Rev. Lett. **21**, 1530 (1968).
[15]D. de Ceglia, M. A. Vincenti, M. Scalora, N. Akozbek, and M. J. Bloemer, AIP Adv. **1**, 032151 (2011).
[16]W. L. Barnes, T. W. Preist, S. C. Kitson, J. R. Sambles, N. P. K. Cotter, and D. J. Nash, Phys. Rev. B **51**, 11164 (1995).
[17]Y. Chu, E. Schonbrun, T. Yang, and K. B. Crozier, Appl. Phys. Lett. **93**, 181108 (2008).
[18]N. Nath and A. Chilkoti, Anal. Chem. **76**, 5370–5378 (2004).
[19]J. W. Chou, K. C. Lin, Y. J. Lee, C. T. Yuan, F. K. Hsueh, H. C. Shih, W. C. Fan, C. W. Luo, M. C. Lin, W. C. Chou, and D. S. Chuu, Nanotechnology **20**, 305202 (2009).
[20]D. Pacifici, H. J. Lezec, H. A. Atwater, and J. Weiner, Phys. Rev. B **77**, 115411 (2008).
[21]J. Garcia-Vidal, L. Martin-Moreno, T. W. Ebbesen, and L. Kuipers, Rev. Mod. Phys. **82**, 729 (2010).
[22]M. Grande, R. Marani, F. Portincasa, G. Morea, V. Petruzzelli, A. D'Orazio, V. Marrocco, D. de Ceglia, and M. A. Vincenti, Sens. Actuators B: Chem. **160**, 1056–1062 (2011).
[23]H. Raether, *Surface Polaritons on Smooth and Rough Surfaces and on Gratings* (Springer, Berlin, 1988).
[24]R. Marani, M. Grande, V. Marrocco, A. D'Orazio, V. Petruzzelli, M. A. Vincenti, and D. de Ceglia, Opt. Lett. **36**, 903–905 (2011).
[25]M. A. Vincenti, D. de Ceglia, M. Scalora, R. Marani, V. Marrocco, M. Grande, G. Morea, and A. D'Orazio, SPIE Proc. **7946**, 794625 (2011).
[26]E. Chow, A. Grot, L. W. Mirkarimi, M. Sigalas, and G. Girolami, Opt. Lett. **29**, 1093–1095 (2004).
[27]N. M. Hanumegowda, C. J. Stica, B. C. Patel, I. M. White, and X. Fan, Appl. Phys. Lett. **87**, 201107 (2005).
[28]C. A. Barrios, K. B. Gylfason, B. Sánchez, A. Griol, H. Sohlström and M. Holgado, Opt. Lett. **32**, 3080–3082 (2007).
[29]M. Sumetsky, R. S. Windeler, Y. Dulashko, and X. Fan, Opt. Express **15**, 14376–14381 (2007).